PCCP

PAPER

View Article Online
View Journal | View Issue

Cite this: *Phys. Chem. Chem. Phys.*, 2014, **16**, 21271

Transient UV pump–IR probe investigation of heterocyclic ring-opening dynamics in the solution phase: the role played by nσ* states in the photoinduced reactions of thiophenone and furanone†

Daniel Murdock,* Stephanie J. Harris, Joel Luke, Michael P. Grubb, Andrew J. Orr-Ewing and Michael N. R. Ashfold*

Received 15th August 2014,
Accepted 20th August 2014

DOI: 10.1039/c4cp03653k

www.rsc.org/pccp

The heterocyclic ring-opening dynamics of thiophenone and furanone dissolved in CH_3CN have been probed by ultrafast transient infrared spectroscopy. Following irradiation at 267 nm (thiophenone) or 225 nm (furanone), prompt ($\tau < 1$ ps) ring-opening is confirmed by the appearance of a characteristic antisymmetric ketene stretching feature around 2150 cm^{-1}. The ring-opened product molecules are formed highly vibrationally excited, and cool subsequently on a ~6.7 ps timescale. By monitoring the recovery of the parent (S_0) bleach, it is found that ~60% of the initially photoexcited thiophenone molecules reform the parent molecule, in stark contrast with the case in furanone where there is less than 10% parent bleach recovery. Complementary *ab initio* calculations of potential energy cuts along the S–C(=O) and O–C(=O) ring-opening coordinate reveals insights into the reaction mechanism, and the important role played by dissociative (n/π)σ* states in the UV-induced photochemistry of such heterocyclic systems.

I. Introduction

The recent literature contains many publications highlighting the critical role played by optically "dark" (n/π)σ* states (*i.e.*, states formed by σ* ← π and σ* ← n electronic excitations where π and n represent bonding and non-bonding orbitals, respectively) in the non-radiative decay of heteroatom containing molecules in the gas phase.[1–3] The diabatic potential energy surfaces (PESs) of electronic states formed by σ* ← n/π excitation will be repulsive with respect to X–Y bond extension (X = O, N, S, *etc.*; Y = H, CH_3, *etc.*). Population of such states thus offers a route to dissociation or internal conversion (IC) *via* conical intersections located at extended X–Y bond distances. This paradigm has been shown to be equally applicable to photodissociation processes in the condensed (solution) phase also. For example, recent time-resolved ultraviolet (UV) pump–broadband UV-visible or infrared (IR) probe studies of thiols, thioanisoles, *etc.*, demonstrate that the characteristics of the bond fission processes that occur under isolated molecule conditions are barely changed in the presence of a weakly interacting solvent such as cyclohexane.[4–6] While the solvent may have minimal impact on the photodissociation process itself, the fate of the photoexcited molecules and/or fragmentation products may be very different in the condensed phase. In particular, additional processes that are unique to the condensed phase may also be observed including (i) vibrational relaxation of the initially excited parent molecules prior to their dissociation and/or of the radical cofragments formed upon X–Y bond fission, and (ii) geminate recombination of the X and Y containing fragments leading to the reformation of the XY parent or isomeric adducts. This latter process is an important step in many photoinitiated organic reactions such as the photo-Claisen and photo-Fries rearrangements.[7–9]

It seems likely that the same (n/π)σ* mediated bond fission should also underpin the photoinduced ring-opening of heterocyclic molecules. Indeed, ring cleavage as a radiationless deactivation pathway has been proposed to account for the ultrafast decay of several heteroatom containing systems including furan,[10–13] thiophene,[14–16] β-glucose,[17] coumarin,[18] various substituted spiropyrans,[19–21] and DNA bases.[22] Direct experimental evidence of ring-opening in such systems is harder to find, however. Part of the reason for this lies in the difficulty of studying these processes in the gas phase. Since the reactant and product

School of Chemistry, University of Bristol, Cantock's Close, Bristol, UK BS8 1TS. E-mail: daniel.murdock@bristol.ac.uk, mike.ashfold@bristol.ac.uk

† Electronic supplementary information (ESI) available: UV absorption spectra of thiophenone/CD_3CN and furanone/dichloromethane. FTIR spectra of thiophenone/CH_3CN and furanone/CH_3CN. Active space used in CASSCF calculations. Calculated harmonic and anharmonic wavenumbers for the parent and product molecules. See DOI: 10.1039/c4cp03653k

molecules are structural isomers, the broad class of experiments that rely upon mass-specific detection schemes are often incapable of distinguishing their signals. Furthermore, the ring-opened products are likely to be formed highly vibrationally excited, where rapid intramolecular vibrational energy redistribution processes will greatly complicate the resulting IR spectra.

Studying the photoinitiated ring-opening of heterocyclic molecules in the condensed phase alleviates many of these problems. The presence of surrounding solvent molecules allows for efficient relaxation of the excess vibrational energy, and enables the reactant and product molecules to be differentiated through their IR spectra.[19,23] The UV induced ring-opening of heterocyclic α-carbonyl systems such as 2(5*H*)-furanone and 2(5*H*)-thiophenone (henceforth furanone and thiophenone) is particularly well suited for detailed mechanistic study by this method, since the ring-opening reaction of this class of molecules should result in the formation of a ketene (C═C═O) moiety, which has an intense and characteristic antisymmetric stretching mode around 2100 cm^{-1}. The ketene vibration has proven itself a valuable marker to gauge the timescales of reaction in previous transient IR studies of photoisomerisation of several molecules including *o*-nitrobenzaldehyde[24,25] and the Wolff rearrangement of diazoketones.[26] Breda and coworkers[27] studied the UV induced unimolecular photochemistry of both furanone and thiophenone isolated within low temperature argon matrices through a combination of Hg lamp irradiation and Fourier transform IR spectroscopy. Both compounds were found to undergo UV-induced α-cleavage, resulting in ring-opened products with an intense ketene peak. Since long irradiation times were used, these experiments provide no dynamical information pertaining to the ring-opening processes. In this paper we extend our recent studies on the dynamics of photodissociation processes in the solution phase to follow the ring-opening reactions of furanone and thiophenone. By using time-resolved infrared (TRIR) spectroscopy to probe the carbonyl (~1700 cm^{-1}) and ketene stretching regions, the timescales and quantum yields for product formation may be followed. Comparing these results with the predictions of *ab initio* calculations of the potential energy curves (PECs) involved in the photochemical transformations reveals features that mediate the dynamics of ring-opening processes in heterocyclic systems.

II. Experimental and computational methodology

The TRIR spectra presented in this paper were recorded on a newly constructed fs-laser transient absorption system at the University of Bristol. The experiment will be described in detail in a future publication, so only the most salient features are discussed here. An amplified Titanium Sapphire laser system generated 800 nm (band center) pulses of 35 fs duration at a 1 kHz repetition rate. A portion of this light was used to pump an optical parametric amplifier (OPA) producing mid-IR radiation of ~300 cm^{-1} bandwidth by difference frequency generation, with the remainder of the 800 nm light sent to another OPA system providing broadly tunable UV pump radiation. The two optical pulses were overlapped in the sample with the transmitted IR radiation being dispersed onto a 128 pixel mercury cadmium telluride (MCT) detector. A second MCT array monitored the intensity of the input IR radiation to allow normalization of the transient signals.

Thiophenone and furanone (98% stated purity) were obtained from Sigma-Aldrich and used without further purification. Thiophenone solutions of 23 mM and furanone solutions of 63 mM concentration were made up in acetonitrile (CH_3CN). The solutions flowed through a Harrick cell fitted with a 100 μm Teflon spacer sandwiched between CaF_2 windows. The concentrations of the solutions were chosen to ensure an optical density of 0.5 at 267 and 225 nm for thiophenone and furanone, respectively, at this pathlength. The experimental response function is limited at early times to ~1 ps due to background noise induced by the cell windows.

Electronic structure calculations were carried out using the Gaussian09[28] and Molpro10[29] computational packages. Ground state structures for the parent, various possible products, and the transition states linking them were optimized at the MP2/6-311+G(d,p) level of theory and their anharmonic vibrational frequencies calculated. The vertical excitation energies were calculated using time dependent density functional theory (TDDFT) coupled with the B3LYP functional and a 6-311+G(d,p) basis. Potential energy cuts were investigated along the S–C(═O) and O–C(═O) bond-breaking coordinate (with all other degrees of freedom allowed to relax to their S_0 minimum values as predicted by non state-averaged complete active space self consistent field (CASSCF) methods) for the ground and first excited $^1A'$ and first two $^1A''$ excited states. These calculations used the state-averaged (SA) CASSCF method. Complete active space with second order perturbation theory (CASPT2) energies were then calculated for all states at these same geometries using the SA-CASSCF result as a reference wavefunction. An imaginary level shift of 0.4 a.u. was included in all CASPT2 calculations to exclude intruder state problems. The SA-CASSCF and CASPT2 calculations employed a reduced 6-31G(d) basis set with an (8,6) active space of eight electrons in six orbitals (shown in the ESI†) comprising the in-plane and out-of-plane lone pair on the central heteroatom (a′ and a″, respectively), two bonding π orbitals (a″), the X–C(═O) σ* orbital (a′) and a π* orbital (a″).

III. Experimental results

A. Thiophenone

Fig. 1 depicts contour plots and accompanying kinetic traces for the results obtained following 267 nm photolysis of a 23 mM solution of thiophenone dissolved in CH_3CN. Two distinct IR probe regions are shown – Fig. 1(a), the region between 1620 and 1720 cm^{-1}, which monitors the carbonyl stretching motions of the parent/product molecules, and Fig. 1(b), the 2000–2220 cm^{-1} region, which allows us to follow any ketene containing products. Fig. 1(a) is dominated by a large negative going signal centered around 1680 cm^{-1}, which reflects the depletion of

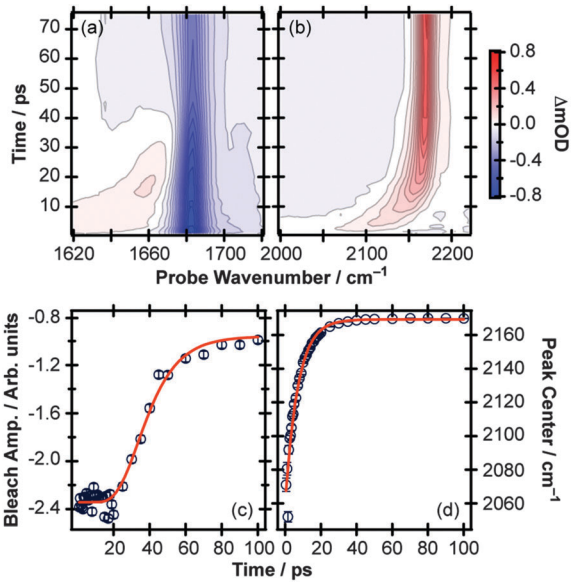

Fig. 1 Transient IR spectra obtained following 267 nm excitation of a 23 mM solution of thiophenone dissolved in CH_3CN, probing (a) the 1620–1720 cm^{-1} range, and (b) the 2000–2220 cm^{-1} range. Decomposition of the region between 1600 and 1720 cm^{-1} in terms of model functions enables a kinetic trace for the bleach amplitude to be extracted (c), with the solid red line being a fit of the data to an analytical function derived from the vibrational relaxation of a harmonic oscillator. (d) Evolution of the antisymmetric ketene stretching mode peak center obtained by fitting each individual time slice to a Lorentzian function. The solid line is a fit to a single rising exponential function.

ground state population induced by the pump pulse. A positive going feature (1600–1670 cm^{-1}) is seen at early pump/probe delays, before decaying away and disappearing completely by ~100 ps. The blue shift and spectral narrowing of this feature as pump/probe time delay increases are characteristic of vibrational cooling. There are two possible sources for this feature, (i) electronically excited parent molecules, and/or (ii) vibrationally excited parent molecules in the ground (S_0) electronic manifold. The observation of a ketene feature at the earliest pump/probe delays investigated (*vide infra*) rules out the possibility of any long lived excited state, so we regard the latter scenario as more likely. The substantial overlap between the vibrationally excited gain and vibrationless bleach signals necessitates that the time resolved spectra be modeled in terms of basis functions in order for their kinetics to be extracted. The signal arising from $S_0(\upsilon > 0)$ molecules was modeled as a sum of two Gaussians, with the respective peak centers and widths obtained from a global fit of all available data, while the amplitudes were allowed to float freely. Since vibrational cooling is expected to be complete within tens of ps, the TRIR spectrum measured at long Δt was used as a guide for the parent bleach signal. The parent bleach amplitude obtained from this fitting procedure is shown in Fig. 1(c) and demonstrates a sigmoidal change with time. The bleach signal remains constant for ~20 ps which we interpret as the time required for the population to cool from highly vibrationally excited levels of the S_0 manifold down to levels with $\upsilon = 1$ before repopulation of the $\upsilon = 0$ level (and accompanying decrease in the bleach signal) can begin. Although only shown for the C=O stretching motion here, all bleaches of the parent molecule vibrational modes should demonstrate the same sigmoidal behaviour. Fitting the extracted bleach amplitude to a model based upon the vibrational relaxation of a harmonic oscillator (detailed in the appendix) results in an estimated rate coefficient of ~0.08 ps^{-1} for the $\upsilon = 1 \rightarrow 0$ step (time constant of 12.5 ps). It is also important to note that the bleach does not recover fully, with the fit suggesting that only ~60% of the initially excited population reforms the parent molecule, indicating that 40% of the thiophenone molecules excited at 267 nm either undergo ring opening or form other (undetected) product molecules.

Fig. 1(b) monitors the build up of any ketene containing molecules – a sign of a ring-opening reaction. A single positive going feature dominates this spectral region, being very broad (~100 cm^{-1}) at the earliest pump/probe time delays measured, before narrowing and blue shifting on a ps timescale. The presence of this feature at very early times indicates that an ultrafast ($\tau < 1$ ps) ring-opening process is occurring following excitation at 267 nm. Fitting each individual time slice to a Lorentzian function monitors the evolution of this feature as a function of pump/probe time delay. The evolution of the extracted peak center as a function of time provides a measure of the average vibrational cooling rate of the ketene containing product molecules. The results of this analysis, along with a fit to a single exponential are shown in Fig. 1(d). The derived lifetime, 6.8(4) ps (where the number in parentheses represents one standard deviation uncertainty in the last significant digit), is comparable with the $\upsilon = 1 \rightarrow 0$ relaxation rate extracted from the fit of the parent bleach dynamics to a simple harmonic oscillator model.

B. Furanone

Contour plots and accompanying kinetic traces obtained following the 225 nm photolysis of a 63 mM solution of furanone dissolved in CH_3CN are shown in Fig. 2. Fig. 2(a) shows the evolution of the carbonyl stretch region of the spectrum (1650–1790 cm^{-1}). Intense parent molecule bleach features centered around 1745 and 1775 cm^{-1} dominate the spectra at all time delays. In contrast to thiophenone, very little signal ascribable to $S_0(\upsilon > 0)$ parent molecules is observed. The greatly reduced degree of spectral overlap allows the bleach kinetics to be extracted through simple numerical integration of the observed signal (Fig. 2(c)). The observed kinetics show an initial increase in the bleach amplitude, likely a result of overlapping positive contributions from vibrationally hot S_0 molecules, before a decrease in signal which may be fit by a single exponential function (for $\Delta t > 7$ ps) revealing a bleach recovery time of 14(3) ps. This time constant is consistent with rapid IC from the initially photoprepared state followed by vibrational cooling on the S_0 PES, ultimately repopulating the $S_0(\upsilon = 0)$ level. The long time recovery of the bleach intensity reveals the quantum yield for parent reformation to be $\phi_{ref} < 0.1$, significantly lower than the value of 0.6 observed for thiophenone.

In addition to the bleach features, an absorption signal centered around 1690 cm^{-1} is also observed. The prompt appearance of

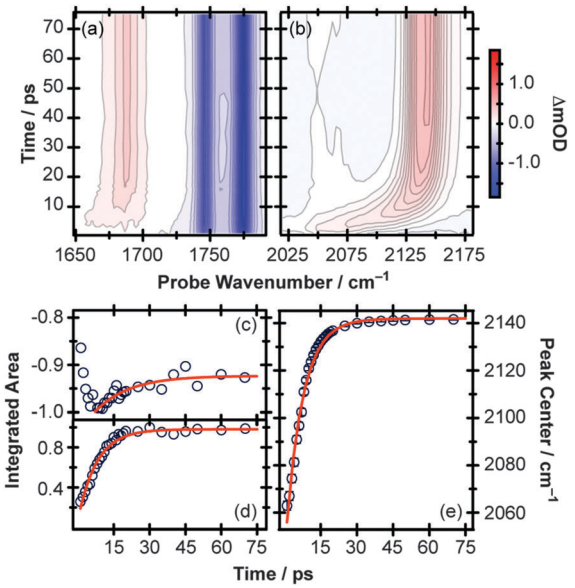

Fig. 2 Transient IR spectra obtained following 225 nm excitation of a 63 mM solution of furanone dissolved in CH_3CN and probing (a) the 1650–1790 cm^{-1} range, and (b) the 2020–2180 cm^{-1} range. (c) Numerical integration over the 1740–1790 cm^{-1} and (d) 1675–1700 cm^{-1} regions allows the evolution of the parent carbonyl bleach and product molecule, respectively, to be monitored, with the solid lines being fits to single exponential functions. (e) Evolution of the antisymmetric ketene stretching mode peak center obtained by fitting each individual time slice to a Lorentzian function. The solid line is a fit to a single rising exponential function.

this feature followed by spectral narrowing is reminiscent of the behavior demonstrated by the ketene formed from thiophenone, and indicates that it is due to product formation rather than being the spectral signature of the initially photo-prepared state. Numerical integration of this feature shows it growing in on an 8.1(5) ps timescale (Fig. 2(d)). The vibrational cooling rate of this feature can be followed in a similar manner to that used for the thiophenone ketene, revealing a time constant of 6.6(3) ps.

Fig. 2(b) shows the results obtained by setting the IR probe to cover the 2020–2180 cm^{-1} range. Just as in thiophenone (Fig. 1(b)), a broad feature ascribed to a ketene moiety is observed at the earliest pump/probe time delays monitored. Again, the prompt appearance of this feature suggests that the initially photo prepared state has a lifetime <1 ps. This feature blue shifts and narrows considerably over the next 30 ps, before reaching its asymptotic wavenumber value of $\sim$2145 cm^{-1} after around 40 ps. Fitting this feature to a Lorentzian lineshape and monitoring the evolution of the peak center as a function of pump/probe time delay enables an average vibrational cooling time of 6.9(2) ps to be extracted (Fig. 2(e)). This rate is consistent with that observed for the 1690 cm^{-1} product peak (Fig. 2(d)), but is faster than that extracted from the parent bleach recovery seen in Fig. 2(c). This latter discrepancy can be explained by considering what we are actually monitoring in each of these kinetic fits; the fit to the bleach is catching the last step of the parent (S_0) vibrational cooling process, while monitoring the growth of the 1690 cm^{-1} feature and the evolution of the ketene band center covers a far wider range of steps down the vibrational ladder of the ring-opened product. Vibrational cooling will be far more rapid for highly vibrationally excited molecules than those in $\upsilon = 1$, therefore, the average cooling rates extracted in Fig. 2(d) and (e) will be shifted to shorter times than those obtained for the $\upsilon = 1 \rightarrow 0$ rate assumed from Fig. 2(c).

IV. Computational results

A. Structures and vertical excitation energies

The S_0 equilibrium geometries of thiophenone and furanone have been optimized at the MP2/6-311+G(d,p) level of theory and are depicted in Fig. 3 and 4, respectively. In agreement with prior microwave[30,31] and computational[32] studies, a planar ring geometry is predicted for both these molecules, resulting in overall C_s symmetry. The vertical excitation energies for the three lowest-lying singlet states of both thiophenone and furanone have been calculated with TDDFT using the B3LYP functional and 6-311+G(d,p) basis set, with the obtained energies and dominant excitation type shown in Fig. 3 and 4. In the case of thiophenone, only the $S_2(n\pi^*)$ state is predicted to have an appreciable oscillator strength ($f = 0.035$), while the $S_2(n\pi^*)$ and $S_3(n\pi^*)$ states in furanone are predicted to have f-values of 0.150 and 0.142, respectively. The predicted energies of the bright states for thiophenone and furanone agree nicely with the experimental UV absorption spectra (shown in the ESI†), which demonstrate absorption maxima at 260 nm (4.77 eV) for thiophenone in CD_3CN, and <220 nm (5.64 eV) for furanone in dichloromethane.

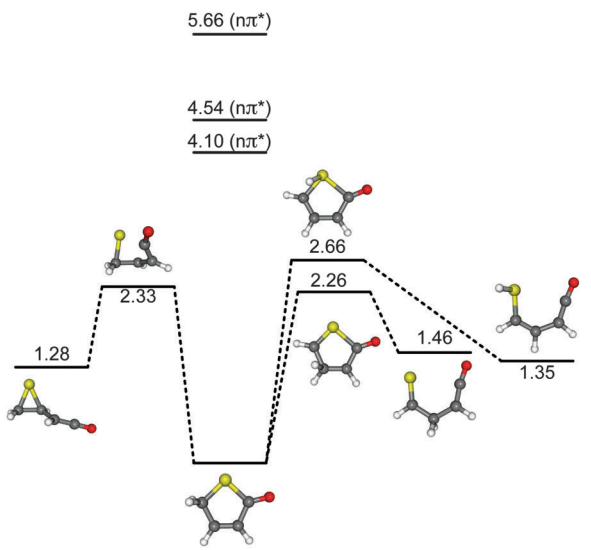

Fig. 3 S_0 equilibrium structure of thiophenone and three possible ring opened product molecules calculated at the MP2/6-311+G(d,p) level of theory. The transition states linking thiophenone to the product molecules have also been calculated, with the pathways being linked by dashed lines. Also shown are the energies and excitation types of the first three electronically excited states of thiophenone calculated at the TD-B3LYP/6-311+G(d,p) level. All energies are in eV and are quoted relative to the equilibrium value of thiophenone.

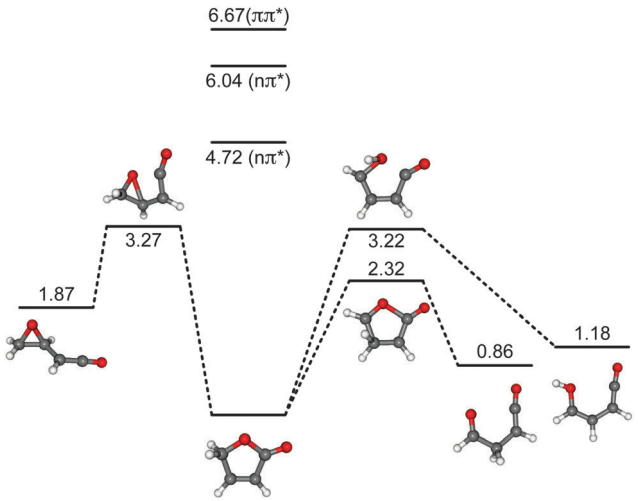

Fig. 4 S_0 equilibrium structure of furanone and three possible ring opened product molecules calculated at the MP2/6-311+G(d,p) level of theory. The transition states linking furanone to the product molecules have also been calculated, with the pathways being linked by dashed lines. Also shown are the energies and excitation types of the first three electronically excited states of furanone calculated at the TD-B3LYP/6-311+G(d,p) level. All energies are in eV and are quoted relative to the S_0 equilibrium value of the parent molecule.

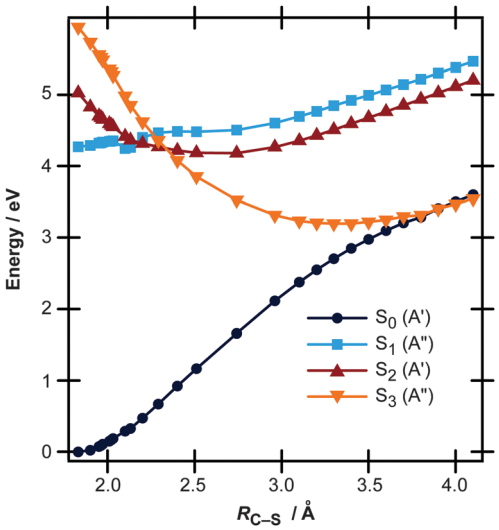

Fig. 5 Cuts along the R_{C-S} ring opening coordinate of the ground, first excited $^1A'$, and first two excited $^1A''$ states of thiophenone calculated at the CASSCF(8,6)/6-31G(d) level with the CASPT2 energy correction applied. For each value of R_{C-S} the rest of the molecular framework was allowed to relax to the S_0 minimum and the vertical excitation energies calculated. The curves have been approximately diabatized to aid in interpretation.

The structures and energies of three possible ring-open products are also shown in Fig. 3 and 4, which, in addition to a ketene moiety, also possess either a (thio)aldehyde, (thio)-epoxy, or (thio)enol functional group. Of these possible end products, both the aldehyde and enol products require a [1,2]-hydrogen atom migration during their formation. Only the aldehyde product (and various conformers thereof) was implicated in the matrix isolation study of Breda and coworkers,[27] but our calculations indicate that other ring-opened forms are energetically accessible and should be considered. The transition states between the parent molecule and these ring-opened products have also been calculated at the MP2/6-311+G(d,p) level of theory (with subsequent vibrational calculations revealing a single imaginary frequency, highlighting the transition-state nature of these structures). The optimized transition state structures are shown in Fig. 3 and 4 along with their energies relative to the respective S_0 minima.

B. Relaxation pathways

i. Thiophenone. The PECs governing the ring cleavage process in thiophenone have been studied in more detail and are shown in Fig. 5. These curves were obtained by elongating the C(=O)–S bond in small increments and allowing the rest of the molecular framework to relax to the S_0 minimum geometry at the CASSCF (8,6)/6-31G(d) level of theory, with C_s symmetry being enforced at each step. The vertical excitation energies of the first excited A′ and first two A″ states were computed by state-averaging the lowest two states of each symmetry together and applying the CASPT2 energy correction. To aid interpretation, it proves convenient to (approximately) diabatize the resultant PECs through inspection of the symmetry, energy, and wavefunction coefficients of the adiabatic states returned by the calculations. The $S_1(A'')$ and $S_2(A')$ states have primarily nπ* character in the vertical Franck–Condon (vFC) region, with $S_3(A'')$ being an nσ* state. Both of the nπ* states display minima at moderate R_{C-S} bond distances, while the S_3 state is repulsive along this coordinate. Curve crossings exist between the $S_2(A')$ and $S_3(A'')$ states at $R_{C-S} \approx 2.5$ Å, and between $S_3(A'')$ and $S_0(A')$ at $R_{C-S} \approx 4.0$ Å. Although transitions between the PESs are symmetry forbidden at these conical intersections, strong vibrational coupling between the states promoted by normal modes of a″ symmetry can be expected to occur, providing a route for the initially excited thiophenone molecules to return to the S_0 potential.

ii. Furanone. As for thiophenone, PECs governing the ring cleavage process in furanone have been studied by elongating the C(=O)–O bond in small increments and optimizing the rest of the molecular framework to its minimum energy geometry in the S_0 state at the CASSCF(8,6)/6-31G(d) level of theory. These surfaces, depicted in Fig. 6, were again obtained while enforcing a planar ring geometry at each step. In the vFC region, $S_1(A'')$ is primarily an nπ* state, $S_2(A')$ is ππ*, while the $S_3(A'')$ state is best described as πσ*. Upon extension of the R_{C-O} ring-coordinate, the energy of the out-of-plane non-bonding orbital on the ring oxygen increases relative to the π orbitals, with the result that at $R_{C-O} = 2.1$ Å the $S_2(A')$ and $S_3(A'')$ states are best described as nπ* and nσ*, respectively. The repulsive S_3 state can be seen to cross S_2 at $R_{C-O} \approx 2.2$ Å and then the S_0 PEC once the C–O bond has extended to 3.2 Å. As before, transitions between the PESs will be symmetry forbidden at these conical intersections, but strong vibrational coupling between the states is likely to be promoted by normal modes of a″ symmetry.

By combining the information gleaned from the TDDFT and CASSCF calculations described above, a picture of the ring-opening

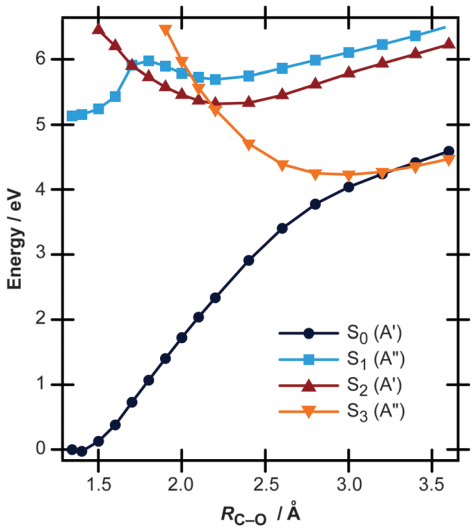

Fig. 6 Cuts along the R_{C-O} ring opening coordinate of the ground, first excited ^{1}A′, and first two excited ^{1}A″ states of furanone calculated at the CASSCF(8,6)/6-31G(d) level with the CASPT2 energy correction applied. For each value of R_{C-O} the rest of the molecular framework was allowed to relax to the S_0 minimum and the vertical excitation energies calculated. The curves have been approximately diabatized to aid in interpretation.

reactions in thiophenone and furanone begins to emerge. A likely mechanism for both molecules at the excitation energies employed in these experimental studies is: (i) initial population of the $S_2(n\pi^*)$ state induced by the 267 and 225 nm radiation, (ii) radiationless transfer onto the $S_3(n\sigma^*)$ PES at $R_{C-S} \approx 2.5$ Å ($R_{C-O} \approx 2.2$ Å), and (iii) repopulation of the S_0 state induced by another conical intersection located at $R_{C-S} \approx 4.0$ Å ($R_{C-O} \approx 3.2$ Å), followed by either reformation of the parent molecule or creation of ring opened product molecules following dynamics on the ground state potential. The sub-ps ring opening observed experimentally accords with the barrierless nature of the electronically excited reaction coordinate predicted upon C–S/C–O bond extension. It is important to note, however, that ring cleavage is unlikely to be the only pathway available for these systems to relax back to the S_0 potential. Recent experimental and computational work on coumarin,[18] which contains a six-membered heterocyclic α-carbonyl moiety, proposes two parallel radiationless relaxation pathways: a ring-opening route similar to the ones discussed in this paper, and a transition *via* a dark state mediated by the carbonyl stretching mode.

In both thiophenone and furanone, the conical intersection linking the S_0 and S_3 states is predicted to lie at higher energy than any of the transition states shown in Fig. 3 and 4. All of the product molecules considered in this paper are thus energetically accessible following ring-opening and subsequent ground state dynamics. The shape of the conical intersection will determine the branching between these various products and the channel leading to repopulation of the ring-closed parent. To help determine which of the possible products is dominant, anharmonic wavenumber calculations at the MP2/6-311+G(d,p) level of theory have been performed for all eight molecules considered in this study (the two parent molecules and the six potential ring-opened products illustrated in Fig. 3 and 4). The results obtained from this vibrational analysis are detailed in the ESI.† In the case of thiophenone, the only product vibration observed experimentally is the antisymmetric ketene stretching mode centered around 2170 cm^{-1}, with the region between 1200 and 1700 cm^{-1} displaying only parent bleach features. The three product molecules are all predicted to show a ketene stretch at ~2155 cm^{-1}, and consequently this spectral region cannot be used to distinguish between them. We run into the same problems when considering furanone, the three product molecules considered all have ketene stretching bands predicted to lie around 2165 cm^{-1}, in good agreement with the experimentally observed value of 2140 cm^{-1}. In contrast to thiophenone, however, the TRIR data from furanone exhibit a second vibrational feature centered around 1690 cm^{-1} attributable to a product molecule. The epoxy-containing molecule is not predicted to have any vibrations in this region, but the aldehyde and enol systems are predicted to exhibit normal modes at 1742 cm^{-1} and 1675 cm^{-1}, respectively. We favor the aldehyde assignment on the basis of its predicted intensity relative to the carbonyl stretching feature of the parent molecule. This assignment is in agreement with that of Breda *et al.* who observed excellent correspondence between their predicted spectrum for the aldehyde (calculated at the B3LYP/6-311++G(d,p) level) and the measured spectrum of their matrix isolated photoproducts, especially in the 500–1500 cm^{-1} region.[27]

Conclusions

The photoinduced ring cleavage reactions of the heterocyclic α-carbonyl systems thiophenone and furanone have been investigated following excitation at 267 and 225 nm, respectively. The application of fs time-resolved infrared spectroscopy allows the evolution of both the parent molecule and photoproducts to be followed in time, with the observation of an antisymmetric ketene stretch providing unequivocal evidence for ring opening in both these systems. Following irradiation, both thiophenone and furanone demonstrate ultrafast (<1 ps) deactivation of the initially excited state, with the quantum yield for parent molecule reformation being ~60% in the case of thiophenone but <10% for furanone. The ring-opened product is formed highly vibrationally excited in both systems, and an average vibrational cooling rate can be obtained by monitoring the evolution of the peak center of the ketene stretch as a function of pump/probe time delay. In a similar manner, population that finds its way back to the parent S_0 state is also highly vibrationally excited. The evolving intensity of the carbonyl bleach signal exhibited by thiophenone is sigmoidal in nature, and has been fit using a qualitative model based upon the vibrational relaxation of a harmonic oscillator. These experimental studies have been accompanied by *ab initio* calculations of the PECs mediating the ring-cleavage reaction. These computational results suggest that the initial excitation of the S_2 state in both molecules is followed by radiationless transfer to an nσ* state which is repulsive along the ring-opening coordinate. A second conical

intersection provides a pathway for the initially photoexcited population to return to the S_0 potential whereupon it can either reform the parent molecule or undergo a [1,2]H-atom shift to form a stable ring-opened product. The barrierless nature of the reaction pathway agrees with the ultrashort excited state lifetime observed experimentally. We do recognize, however, that the present (C_s constrained) calculations do not allow us to rule out the possible existence of alternative non-planar conical intersections, which would enable the IC and [1,2]H-atom shift to occur in a concerted rather than stepwise fashion. The detailed identities of the ring-opened product molecules are uncertain, with several possibilities considered for both thiophenone and furanone. The branching ratio between the ring-closed and various ring-open forms in each case will be sensitively dependent on the shape of the final conical intersection(s) linking the S_3 and S_0 PESs, and it is envisaged that future computational investigations will allow further refinement of our understanding of these prototypical photo-induced (n/π)σ*-mediated ring opening reactions and subsequent ground state dynamics.

Appendix

The vibrational cooling dynamics of polyatomic molecules in solution is a complex problem. In general, it can be separated into two steps:[33] (i) intramolecular vibrational redistribution, and (ii) intermolecular energy transfer from the solute to the solvent, where both of these processes are mediated by anharmonic (both diagonal and off-diagonal) couplings. Oftentimes experimentally determined anharmonic coupling constants are unavailable, and their calculation is a time-consuming endeavour. In this paper, we have applied a simple model based upon the vibrational dynamics of a harmonic oscillator to explain the delayed onset of the bleach recovery in the parent carbonyl band of thiophenone (Fig. 1c). Despite the many approximations inherent in this approach, it provides a first-order justification for the observed kinetics.

In this model, vibrational cooling is approximated as a linear chain of first-order decay processes involving varying quanta of a single normal mode, $X_1 \rightarrow X_2 \rightarrow \ldots \rightarrow X_m \rightarrow \ldots \rightarrow X_n$, where X_m are vibrational energy levels and each step in the decay chain has a rate coefficient k_m. Setting up and solving a system of first-order linear differential equations allows the time-dependent population of any vibrational level, N_m, in this chain to be obtained:

$$\frac{\mathrm{d}N_m(t)}{\mathrm{d}t} = k_{m-1}N_{m-1}(t) - k_mN_m(t) \tag{A.1}$$

Bateman[34] established a general analytical solution to the above system of differential equations, which, in the limiting case of N_1 being the only non-zero population at time $t = 0$, can be written as:[35]

$$N_m(t) = \frac{N_1(0)}{k_m}\sum_{i=1}^{m} k_i\alpha_i\mathrm{e}^{(-k_it)};\ \alpha_i = \prod_{\substack{j=1\\ j\neq i}}^{m}\frac{k_j}{k_j - k_i} \tag{A.2}$$

The differential equation defining the population of the final level in the decay chain, N_n, is:

$$\frac{\mathrm{d}N_n(t)}{\mathrm{d}t} = k_{n-1}N_{n-1}(t) \tag{A.3}$$

This can be integrated readily

$$\begin{aligned} N_n(t) &= k_{n-1}\int_0^t N_{n-1}(t)\mathrm{d}t \\ &= k_{n-1}\int_0^t \frac{N_1(0)}{k_{n-1}}\sum_{i=1}^{n-1} k_i\alpha_i\mathrm{e}^{-k_it}\mathrm{d}t \\ &= N_1(0)\left\{\sum_{i=1}^{n-1}\alpha_i - \sum_{i=1}^{n-1}\alpha_i\mathrm{e}^{-k_it}\right\} \end{aligned} \tag{A.4}$$

For the special case of a decay chain of harmonic oscillators, $k_{\nu\rightarrow\nu-1} \propto \nu$,[36] resulting in $k_i = (n - i)k$, where k is the rate coefficient for the $1 \rightarrow 0$ vibrational transition and n is the number of vibrational levels in the decay chain. This allows α_i to be rewritten as:

$$\begin{aligned} \alpha_i &= \prod_{\substack{j=1\\ j\neq i}}^{n-1}\frac{(n-j)k}{(n-j)k - (n-i)k} \\ &= \prod_{\substack{j=1\\ j\neq i}}^{n-1}\frac{(n-j)}{(i-j)} \end{aligned} \tag{A.5}$$

which, after some algebra, reduces to:

$$\alpha_\ell = (-1)^{n+\ell}\frac{(n-1)!}{(n-1-\ell)!\ell!} = (-1)^{n+\ell}\binom{n-1}{\ell} \tag{A.6}$$

where $\binom{n}{k}$ is a binomial coefficient defined by $\frac{n!}{(n-k)!k!}$, and $\ell = i - 1$.

Inserting eqn (A.6) into (A.4) and rearranging yields:

$$N_n(t) = N_1(0)\left\{\begin{array}{l} (-1)^n\sum_{\ell=0}^{n-2}(-1)^\ell\binom{n-1}{\ell} \\ \\ +(-1)^{n-1}\sum_{\ell=0}^{n-2}(-1)^\ell\binom{n-1}{\ell}\mathrm{e}^{-(n-1-\ell)kt} \end{array}\right\} \tag{A.7}$$

By using various properties of binomial coefficients, eqn (A.7) can be rewritten as:

$$N_n(t) = N_1(0)\left\{\mathrm{e}^{-(n-1)kt}\left(\mathrm{e}^{kt} - 1\right)^{n-1}\right\} \tag{A.8}$$

Thus, the recovery rate of the $\upsilon = 0$ level can be defined in terms of a single rate coefficient. The results obtained by fitting the thiophenone carbonyl bleach amplitude (from Fig. 1) to eqn (A.8) are shown in Fig. 7. By increasing the number of vibrational levels considered in the fit (through n), the extracted rate coefficient, k, begins to converge to $\sim$0.08 ps^{-1}; the convergence is slow, however, and large values for n have to be considered highlighting the limitations of this approach. Despite this, treating the vibrational cooling as being purely

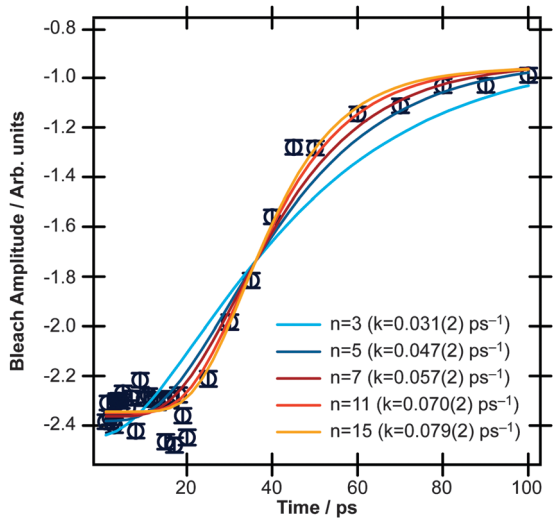

Fig. 7 Fit of eqn (A.8) for differing values of n to the time-evolving thiophenone carbonyl bleach amplitude. The extracted rate coefficients along with their one standard deviation errors are in parentheses.

harmonic in nature succeeds in reproducing the time invariance of the early time signal and allows a qualitative picture of the cooling rate to be obtained.

Acknowledgements

This work was supported by the European Research Council through the ERC Advanced Grant 290966 CAPRI and EPSRC *via* Programme Grants EP/G00224X and EP/L005913. The authors thank Professor Jeremy N. Harvey for help and advice with the DFT and CASSCF calculations.

Notes and references

1 A. L. Sobolewski, W. Domcke, C. Dedonder-Lardeux and C. Jouvet, *Phys. Chem. Chem. Phys.*, 2002, **4**, 1093–1100.
2 M. N. R. Ashfold, B. Cronin, A. L. Devine, R. N. Dixon and M. G. D. Nix, *Science*, 2006, **312**, 1637–1640.
3 M. N. R. Ashfold, G. A. King, D. Murdock, M. G. D. Nix, T. A. A. Oliver and A. G. Sage, *Phys. Chem. Chem. Phys.*, 2010, **12**, 1218–1238.
4 S. J. Harris, D. Murdock, Y. Zhang, T. A. A. Oliver, M. P. Grubb, A. J. Orr Ewing, G. M. Greetham, I. P. Clark, M. Towrie, S. E. Bradforth and M. N. R. Ashfold, *Phys. Chem. Chem. Phys.*, 2013, **15**, 6567–6582.
5 D. Murdock, S. J. Harris, T. N. V. Karsili, G. M. Greetham, I. P. Clark, M. Towrie, A. J. Orr Ewing and M. N. R. Ashfold, *J. Phys. Chem. Lett.*, 2012, **3**, 3715–3720.
6 Y. Zhang, T. A. A. Oliver, M. N. R. Ashfold and S. E. Bradforth, *Faraday Discuss.*, 2012, **157**, 141–163.
7 S. Lochbrunner, M. Zissler, J. Piel, E. Riedle, A. Spiegel and T. Bach, *J. Chem. Phys.*, 2004, **120**, 11634.
8 I. Iwakura, A. Yabushita, J. Liu, K. Okamura and T. Kobayashi, *Phys. Chem. Chem. Phys.*, 2012, **14**, 9696.
9 S. J. Harris, D. Murdock, M. P. Grubb, G. M. Greetham, I. P. Clark, M. Towrie and M. N. R. Ashfold, *Chem. Sci.*, 2014, **5**, 707–714.
10 M. Stenrup and Å. Larson, *Chem. Phys.*, 2011, **379**, 6–12.
11 E. V. Gromov, C. Léveque, F. Gatti, I. Burghardt and H. Köppel, *J. Chem. Phys.*, 2011, **135**, 164305.
12 E. V. Gromov, A. B. Trofimov, F. Gatti and H. Köppel, *J. Chem. Phys.*, 2010, **133**, 164309.
13 N. Gavrilov, S. Salzmann and C. M. Marian, *Chem. Phys.*, 2008, **349**, 269–277.
14 M. Stenrup, *Chem. Phys.*, 2012, **397**, 18–25.
15 G. Cui and W. Fang, *J. Phys. Chem. A*, 2011, **115**, 11544–11550.
16 S. Salzmann, M. Kleinschmidt, J. Tatchen, R. Weinkauf and C. M. Marian, *Phys. Chem. Chem. Phys.*, 2008, **10**, 380–392.
17 D. Tuna, A. L. Sobolewski and W. Domcke, *Phys. Chem. Chem. Phys.*, 2014, **16**, 38–47.
18 C. M. Krauter, J. Möhring, T. Buckup, M. Pernpointner and M. Motzkus, *Phys. Chem. Chem. Phys.*, 2013, **15**, 17846–17861.
19 M. Rini, A.-K. Holm, E. T. J. Nibbering and H. Fidder, *J. Am. Chem. Soc.*, 2003, **125**, 3028–3034.
20 F. Liu and K. Morokuma, *J. Am. Chem. Soc.*, 2013, **135**, 10693–10702.
21 S. Prager, I. Burghardt and A. Dreuw, *J. Phys. Chem. A*, 2014, **118**, 1339–1349.
22 S. Perun, A. L. Sobolewski and W. Domcke, *Chem. Phys.*, 2005, **313**, 107–112.
23 E. T. J. Nibbering, H. Fidder and E. Pines, *Annu. Rev. Phys. Chem.*, 2005, **56**, 337–367.
24 S. Laimgruber, W. J. Schreier, T. Schrader, F. Koller, W. Zinth and P. Gilch, *Angew. Chem., Int. Ed.*, 2005, **44**, 7901–7904.
25 T. Schmierer, W. J. Schreier, F. O. Koller, T. E. Schrader and P. Gilch, *Phys. Chem. Chem. Phys.*, 2009, **11**, 11596–11607.
26 G. Burdzinski, J. Kubicki, M. Sliwa, J. Réhault, Y. Zhang, S. Vyas, H. L. Luk, C. M. Hadad and M. S. Platz, *J. Org. Chem.*, 2013, **78**, 2026–2032.
27 S. Breda, I. Reva and R. Fausto, *Vib. Spectrosc.*, 2009, **50**, 57–67.
28 M. J. Frisch, G. W. Trucks, H. B. Schlegel, G. E. Scuseria, M. A. Robb, J. R. Cheeseman, G. Scalmani, V. Barone, B. Mennucci, G. A. Petersson, H. Nakatsuji, M. Caricato, X. Li, H. P. Hratchian, A. F. Izmaylov, J. Bloino, G. Zheng, J. L. Sonnenberg, M. Hada, M. Ehara, K. Toyota, R. Fukuda, J. Hasegawa, M. Ishida, T. Nakajima, Y. Honda, O. Kitao, H. Nakai, T. Vreven, J. A. Montgomery, J. E. Peralta, F. Ogliaro, M. Bearpark, J. J. Heyd, E. Brothers, K. N. Kudin, V. N. Staroverov, R. Kobayashi, J. Normand, K. Raghavachari, A. Rendell, J. C. Burant, S. S. Iyengar, J. Tomasi, M. Cossi, N. Rega, J. M. Millam, M. Klene, J. E. Knox, J. B. Cross, V. Bakken, C. Adamo, J. Jaramillo, R. Gomperts, R. E. Stratmann, O. Yazyev, A. J. Austin, R. Cammi, C. Pomelli, J. W. Ochterski, R. L. Martin, K. Morokuma, V. G. Zakrzewski, G. A. Voth, P. Salvador, J. J. Dannenberg, S. Dapprich, A. D. Daniels, Ö. Farkas, J. B. Foresman, J. V. Ortiz, J. Cioslowski and D. J. Fox, *Gaussian 09, Revision B.01*, Gaussian, Inc., Wallingford CT, 2009.

29 H.-J. Werner, P. J. Knowles, R. Lindh, F. R. Manby, M. Schütz, P. Celani, T. Korona, A. Mitrushenkov, G. Rauhut, T. B. Adler, R. D. Amos, A. Bernhardsson, A. Berning, D. L. Cooper, M. J. O. Deegan, A. J. Dobbyn, F. Eckert, E. Goll, C. Hampel, G. Hetzer, T. Hrenar, G. Knizia, C. Köppl, Y. Liu, A. W. Lloyd, R. A. Mata, A. J. May, S. J. McNicholas, W. Meyer, M. E. Mura, A. Nicklass, P. Palmieri, K. Pflüger, R. Pitzer, M. Reiher, U. Schumann, H. Stoll, A. J. Stone, R. Tarroni, T. Thorsteinsson, M. Wang and A. Wolf, *MOLPRO, version 2010.1, A Package of Ab Initio Programs*, 2010.
30 A. G. Lesarri, J. C. López and J. L. Alonso, *J. Mol. Struct.*, 1992, **273**, 123–131.
31 J. L. Alonso and A. C. Legon, *J. Chem. Soc., Faraday Trans. 2*, 1981, **77**, 2191–2201.
32 S. Breda, I. Reva and R. Fausto, *J. Mol. Struct.*, 2008, **887**, 75–86.
33 P. Hamm, S. M. Ohline and W. Zinth, *J. Chem. Phys.*, 1997, **106**, 519–529.
34 H. Bateman, *Proc. Cambridge Philos. Soc.*, 1910, **15**, 423–427.
35 J. Cetnar, *Ann. Nucl. Energy*, 2006, **33**, 640–645.
36 J. C. Owrutsky, D. Raftery and R. M. Hochstrasser, *Annu. Rev. Phys. Chem.*, 1994, **45**, 519–555.